ELSEVIER

Thermochimica Acta 269/270 (1995) 649–663

thermochimica acta

A thermoanalytical study of some zinc-fuelled binary pyrotechnic systems ☆

Michael J. Tribelhorn, Dean S. Venables, Michael E. Brown *

Chemistry Department, Rhodes University, Grahamstown, 6140, South Africa

Received 16 September 1994; accepted 16 November 1994

Abstract

Results are reported of a thermoanalytical study of several binary pyrotechnic systems using zinc as fuel and one of the oxidants: PbO_2, Pb_3O_4, PbO, BaO_2, SrO_2 or $KMnO_4$, including estimates of kinetic parameters. These studies show that reactions of zinc with the solid oxidants, under the controlled heating rate conditions of thermal analysis, all involve prior melting of the zinc. Under the uncontrolled conditions of combustion, reaction probably also involves the participation of zinc vapour.

Keywords: Binary system; Pyrolysis; TA; Zinc

1. Introduction

Thermal analysis has been used extensively [1] for studying the processes which occur when small samples of pyrotechnic compositions are heated under controlled conditions. Very little has been published on the use of Zn as a fuel in pyrotechnic delays, although the use of Zn in smoke-producing compositions has been investigated. These systems include Zn/$KClO_4$/hexachlorobenzene [2] and Zn/TNT/hexachloroethane [3].

In an inert atmosphere, Zn melts at 419.5 °C and has a standard boiling point [4] of 908 °C. Its vapour pressure is significant well below this temperature, e.g. 100 mmHg at 730 °C; 400 mmHg at 840 °C [5].

In dry O_2 atmospheres at 25 °C, the layer of ZnO formed on a zinc surface is typically 50–200 nm thick [6]. Above 370 °C, the rate of oxidation is related to temperature and

☆ Presented at the 6th European Symposium on Thermal Analysis and Calorimetry, Grado, Italy, 11–16 September 1994.

* Corresponding author.

SSDI 0040-6031(95)02359-3

pressure by a complex parabolic rate law [7]. Values from 104 to 119 kJ mol^{-1} have been reported [6, 8, 9] for the activation energy of oxidation of zinc by gaseous oxygen.

In the presence of other metal oxides, mixed metal–zinc oxides form readily, e.g. $BaZnO_2$ [10, 11] and $SrZnO_2$ [12] form between 1000 and 1400°C.

The oxidants used in this study, excluding PbO, i.e. PbO_2, Pb_3O_4, BaO_2, SrO_2 and $KMnO_4$, decompose on heating, without melting, to oxygen gas and a solid residue. PbO_2 decomposes [13, 14] via a number of intermediate products to Pb_3O_4, which then decomposes to PbO. Gallibrand and Halliwell [14] showed that the temperatures at which these decomposition steps occurred varied with the composition and structural modification of the sample and its method of preparation. Decomposition of PbO_2 to Pb_3O_4 started between 490 and 540°C, although Pb_3O_4 was sometimes only present in trace quantities. The decomposition to PbO usually occurred at about 590°C and was complete between 600 and 700°C.

PbO may exist as the red tetragonal form (litharge), which is stable below 488°C, or as yellow orthorhombic massicot. Massicot may be stabilised at lower temperatures by the presence of impurities. Well-annealed PbO (melting point 886°C) is thermally stable in non-oxidising atmospheres, but in the presence of oxygen it reacts exothermally to form Pb_3O_4, which then decomposes endothermally back to PbO above 540°C.

Barium peroxide decomposes [15] endothermally above 500°C to BaO(s) and oxygen, and the decomposition of strontium peroxide [15] to SrO(s) occurs in two endothermic stages (onsets at about 390 and 525°C), proposed [16] to be the formation of a layer of a solid solution of oxygen in SrO_2

$$SrO_2(s) \rightarrow SrO(s) + O(ads)$$

$$O(ads) + SrO_2(s) \rightarrow SrO(s) + O_2(g)$$

Onset temperatures are dependent upon the partial pressure of oxygen. Decomposition of peroxides is accelerated in the presence [17] of H_2O and CO_2, and also in the presence of metal oxides [18].

The thermal decomposition of $KMnO_4$ occurs in two steps [19, 20]. The first step is exothermic (onset about 290°C, mass loss 12.15%), and the second step endothermic (onset about 520°C, further 1.82% mass loss of the original sample)

$$10KMnO_4(s) \rightarrow [2.6K_2MnO_4 + (2.3K_2O, 7.3MnO_{2.05})](s) + 6O_2(g)$$

$$10K_2MnO_4(s) \rightarrow [5.7K_3MnO_4 + 0.5(2.9K_2O, 8.6MnO_{2.01})](s) + 3.4O_2(g)$$

From the behaviour described above, the reactions of the zinc/oxidant pyrotechnic mixtures can be expected to include contributions from solid–solid, liquid–solid, liquid–gas, solid–gas and even gas–gas interactions.

2. Experimental

2.1. Materials

The materials used were zinc powder (< 5 μm, 94% pure), lead dioxide (< 75 μm), and red lead (< 75 μm), all supplied by AECI Ltd. Yellow lead monoxide (massicot)

(< 250 μm) was supplied by BDH Ltd. Barium peroxide (85% pure, < 20 μm) was obtained from Saarchem, and strontium peroxide (88% pure, < 20 μm) from Bernardy Chemie, France. $KMnO_4$ powder (< 53 μm) was supplied by AECI Ltd. Mixtures were prepared by tumbling in the presence of rubber balls for 1 h. The compositions of fuel/oxidant mixtures are described in terms of the mass percentage of fuel. Most samples were in powder form. Compacted pellets tended to shatter when heated, unless the amount of sample was very small.

The particle-size distribution of the zinc powder was determined by scanning electron microscopy (SEM), which showed that the zinc consisted largely of small spheres of less than 4 μm diameter, together with a few large agglomerates which were about 10 μm in diameter. The mean diameter of the particles was approx. 1.0 μm.

2.2. Apparatus

A Perkin-Elmer Delta Series 7 thermobalance and differential scanning calorimeter, and a Perkin-Elmer DTA 1700 high-temperature differential thermal analyser were used. The TG furnace was calibrated using the Curie points of nickel (354°C) and iron (780°C). Platinum sample pans without covers were used for TG and aluminium pans with lids for DSC. Difficulties encountered in removing traces of oxygen from the balance housing, and problems experienced with static on the balance whenever $KMnO_4$ was present, have been described [21]. All TG, DSC and DTA runs were performed at heating rates of 20°C min^{-1} in atmospheres of nitrogen or air flowing at 50 cm^3 min^{-1}. The TG range was 100–685°C, the DSC range 100–575°C and the DTA range 100–780°C, unless stated otherwise. (These limits were imposed owing to excessive vaporisation of zinc above 650°C.)

3. Results and discussion

3.1. Zinc powder

The DTA curve of zinc in nitrogen (Fig. 1, curve a) shows a sharp melting endotherm (onset 420°C) and a broad vaporisation endotherm (onset 685°C). The DTA curve in air (Fig. 1, curve b) shows that the melting endotherm is followed immediately by a broad exotherm attributable to the oxidation of the metal.

The TG curve in air (Fig. 2, curve b) confirmed the onset of the oxidation at 420°C. Oxidation was incomplete at 850°C (the maximum operating temperature of the instrument) at which stage a mass gain of almost 23% had been observed (24.5% calculated for $Zn \rightarrow ZnO$, but considering 94% pure zinc, a 23.0% gain is expected). The maximum rate of oxidation was at about 575°C. The DTG curve in air (Fig. 2, curve c) is very similar to the DTA curve in air (Fig. 1, curve b). The TG curve in N_2 (Fig. 2, curve a) shows onset of significant vaporisation above 550°C.

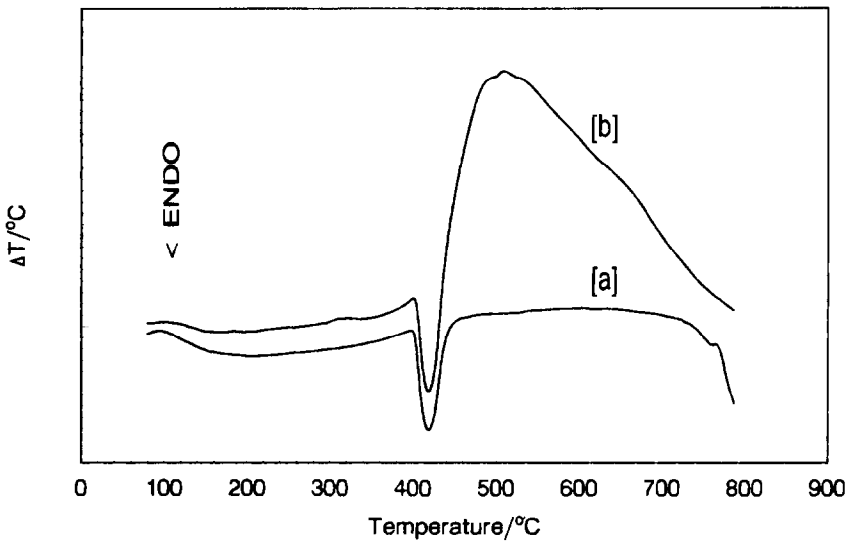

Fig. 1. DTA of Zn powder heated at 20°C min^{-1}: (a) in N_2; (b) in air.

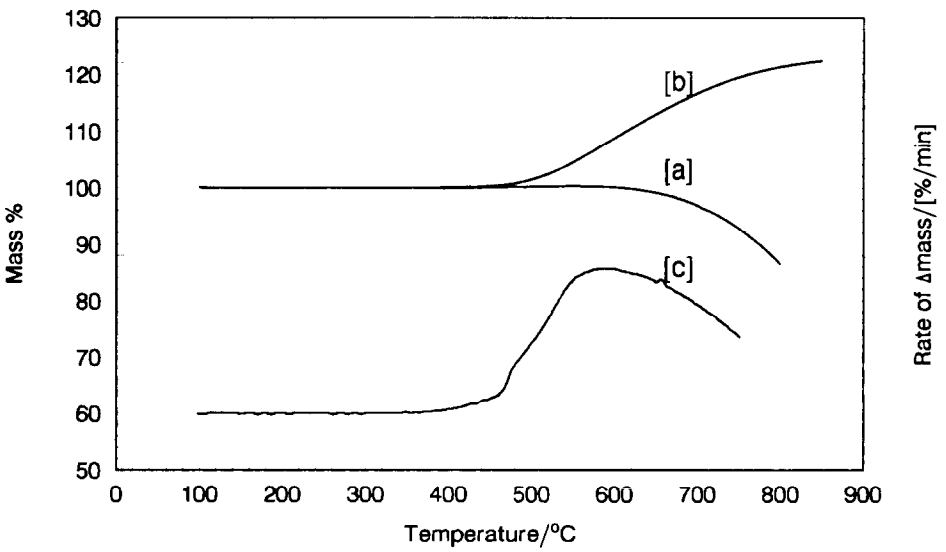

Fig. 2. TG of Zn powder heated at 20°C min^{-1}: (a) in N_2; (b) in air; (c) DTG in air.

3.2. *Characterisation of the oxidants*

PbO_2

DTA curves of PbO_2 in air and nitrogen showed a number of shallow, poorly defined endotherms between 320 and 600°C. TG curves showed two overlapping stages over

the temperature range 370–570°C; the mass loss in the first step corresponds approximately to the decomposition $PbO_2 \rightarrow Pb_3O_4$, and in the second step to $Pb_3O_4 \rightarrow PbO$. The overall mass loss was consistent with the overall decomposition of PbO_2 to PbO (experimental and calculated both 6.69%).

Pb_3O_4

DTA curves showed that the endothermic decomposition of Pb_3O_4 occurred at about 560°C in nitrogen, and at about 580°C in air. Two small endotherms, visible between 270 and 380°C, may be caused by the decomposition of residual impurities, most probably PbO_2. TG curves in nitrogen revealed a small loss in mass at 350°C which corresponds to the onset of PbO_2 decomposition, confirming its presence as an impurity. The decomposition of Pb_3O_4 occurred in a single step starting from 550°C, with a loss in mass of 2.19%. (Calculated for $Pb_3O_4 \rightarrow PbO$, 2.33%.)

PbO

DTA curves of PbO in air and nitrogen show two small endotherms at 280 and 330°C, accompanied by a small loss in mass. TG curves of PbO in air did not show any gain in mass indicating the expected formation of Pb_3O_4. This may be related to the presence of $PbCO_3$ on the surface of the sample, which could isolate PbO from the atmosphere.

BaO_2

TG curves for BaO_2 heated in N_2 at 20°C min^{-1} showed the removal of small amounts (0.2%) of moisture at about 100°C, onset of decomposition above 500°C, and maximum decomposition rate at about 580°C. The 7.7% mass loss found agrees well with the expected loss of 8.0% for decomposition of 85% pure BaO_2 to BaO and O_2. In O_2, onset of decomposition was shifted to about 650°C and the maximum rate to 680°C.

SrO_2

On heating SrO_2 in nitrogen, small amounts of moisture were removed at about 100°C. Subsequent decomposition occurs in two consecutive steps. The first stage is accompanied by a mass loss of 3.8% (onset 390°C) followed by a loss of a further 7.7% (onset 525°C). A further gradual loss of 2% occurs towards the limit of the instrument at 900°C. The calculated mass loss for decomposition of 85% pure SrO_2 to SrO and O_2 is 11.4%. The mass loss at high temperature probably corresponds to the decomposition of some $SrCO_3$ present in the reactant. In O_2, the relative mass losses in the two stages are different: 8–9% for the first stage followed by 3–4% in the second. The onset temperatures are dependent on the partial pressure of O_2(g).

$KMnO_4$

The sample of $KMnO_4$ used showed the normal two-step decomposition [19, 20] (exothermic, onset 290°C, mass loss 12.25%; then endothermic, onset 520°C, mass loss about 3.5%).

3.3. The pyrotechnic systems

A common feature in all DTA curves was the melting of Zn at 420°C. One or two exotherms followed the melting of Zn. In air, the reaction of Zn with atmospheric oxygen appeared as an exotherm shortly after the fusion of Zn, obscuring the reaction of Zn with the oxidant in some systems.

Zn/PbO

A 30% Zn/PbO composition heated in nitrogen gave the DTA curve shown in Fig. 3. The small endotherm at about 330°C is observed in the DTA curves of PbO. A broad exotherm (onset 540°C) appeared after the fusion of Zn. The slight shoulder at about 610–630°C also appears in the DTA curves of Zn/PbO_2 and Zn/PbO_4 mixtures. Exotherms similar in size, position and shape were observed in air indicating that there is little or no contribution to reaction from atmospheric oxygen.

Zn/Pb_3O_4

DTA curves of Zn/Pb_3O_4 in nitrogen showed a single, sharp exotherm starting at about 580°C (Fig. 4). The formation of ZnO from the slower reaction of Zn and atmospheric oxygen has onset at about 530°C which is before the main exotherm at 580°C. Reaction therefore probably arises from the reaction of liquid Zn with decomposing Pb_3O_4.

Zn/PbO_2

The reaction of Zn with PbO_2 in nitrogen is similar to that with Pb_3O_4 in terms of the shape and position of the reaction exotherm (Fig. 5) at about 580°C. The same

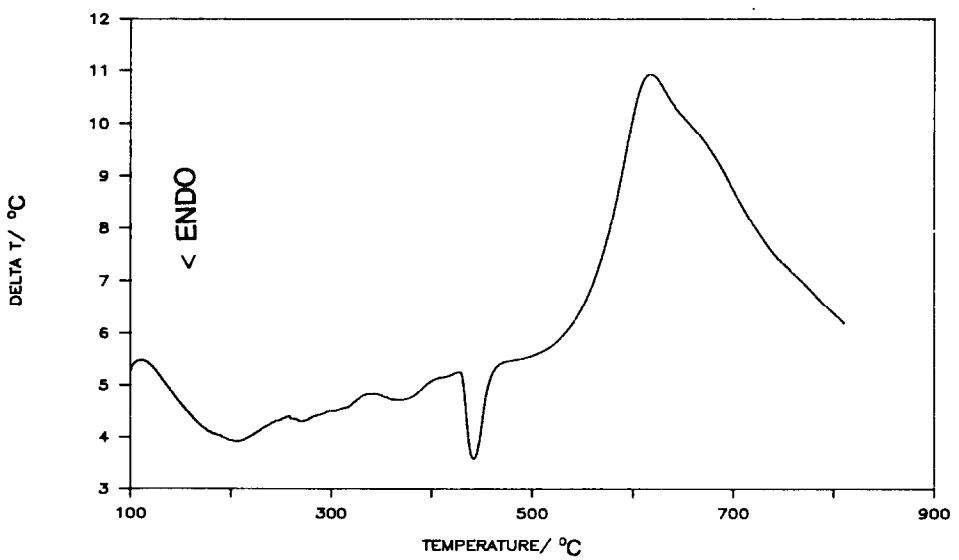

Fig. 3. DTA of 30% Zn/PbO heated in N_2 at 20°C min^{-1}.

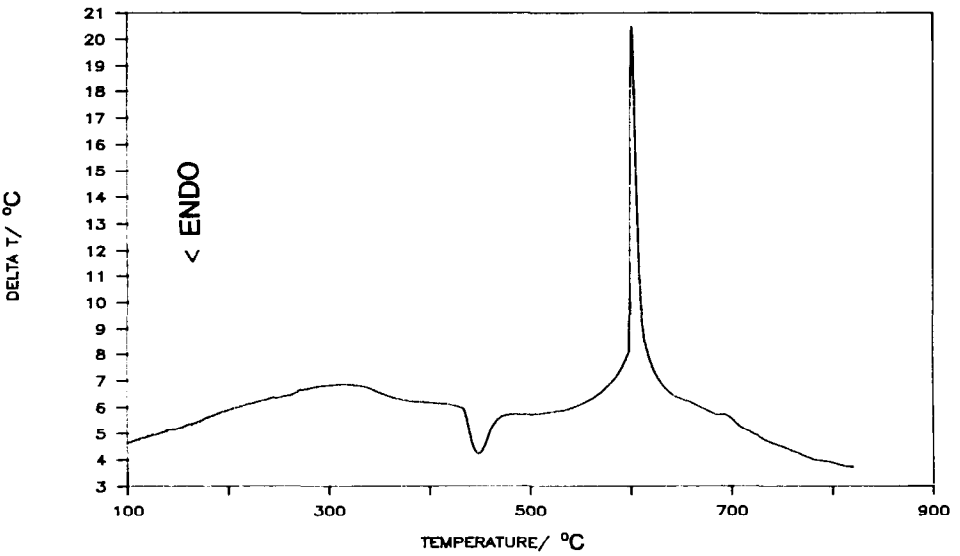

Fig. 4. DTA of 30% Zn/Pb_3O_4 heated in N_2 at 20°C min^{-1}.

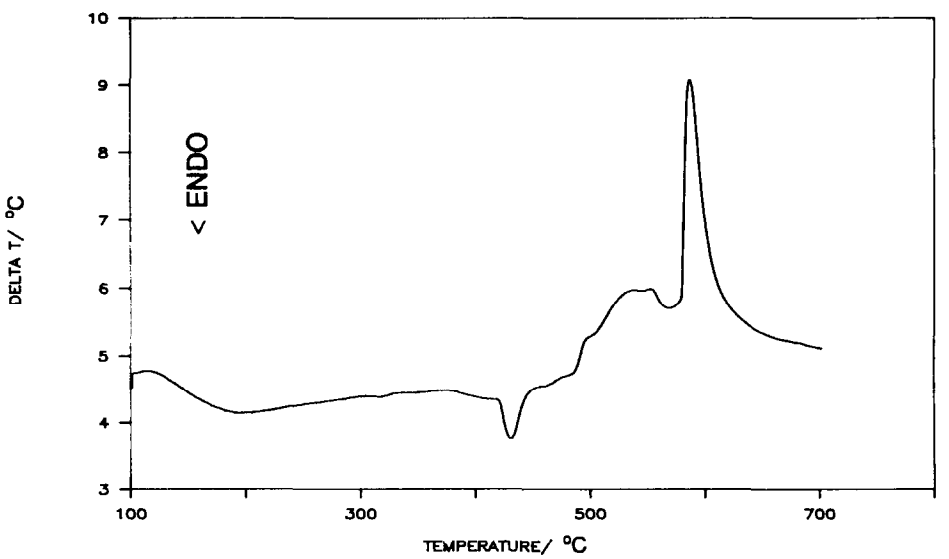

Fig. 5. DTA of 30% Zn/PbO_2 heated in N_2 at 20°C min^{-1}.

reaction is probably taking place in both systems, namely, the reaction of liquid Zn with decomposing Pb_3O_4 (to which PbO_2 has fully decomposed by about 570°C). Similar results have been reported by Yoganarasimhan et al. [22] using Ta as the fuel. PbO_2 forms a more active Pb_3O_4 than the well-annealed Pb_3O_4 used as the oxidant, and thus

fuel/PbO_2 mixtures are generally more likely to sustain combustion than fuel/Pb_3O_4 mixtures. The decomposition of PbO_2 may also release gaseous oxygen into the interstices of the mixture, and diffusion of Zn into the oxidant lattice may occur more readily during the decomposition of PbO_2.

Zn/BaO_2

The DTA curves for 30% Zn/BaO_2, heated at 20°C min^{-1} in N_2 (Fig. 6, curve c), showed the melting of zinc at 418°C, followed immediately by a complex exotherm with a maximum at about 495°C. In air (Fig. 6, curve d), the complex exotherm was partially resolved into three main peaks with onset temperatures at approximately 420, 510 and 560°C. The behaviour of the 30% mixture is very different to the reaction of molten Zn in air and O_2. The DTA curves for Zn in air (curve a) and BaO_2 in N_2 (curve b) are shown on the same scale for comparison. DSC results were similar. Pelleting the sample consolidated and sharpened the exotherms.

After the initial melting endotherm at 420°C, the 50% Zn/BaO_2 mixture gave a broad exotherm (onset 420°C) followed by a sharp exotherm (onset 560°C) in N_2. In O_2, the trace of the 50% system did not show the sharp exotherm at 560°C.

For the 30% Zn/BaO_2 composition, if no external reaction occurred, the overall mass change would be zero and 76.5% of the Zn would be oxidised. Independent oxidation of the 30% Zn (94% pure) and decomposition of the 70% BaO_2 (85% pure) would result in a net mass increase of 1.3%. The TG curve for 30% Zn/BaO_2, heated at 20°C min^{-1} in N_2 (Fig. 7, curve c) showed a mass loss with onset at 600°C, extending to beyond the instrument range of 700°C. In air, the mass loss was shifted to higher temperatures (onset 725°C) indicating that reaction was occurring with significant atmospheric interference. Two types of behaviour were evident in both 30 and 50%

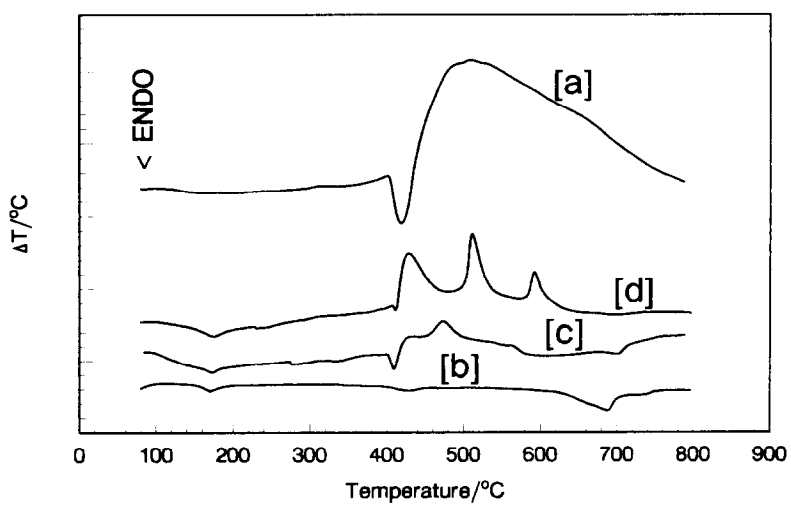

Fig. 6. DTA curves for 30% Zn/BaO_2 heated at 20°C min^{-1}; (a) Zn powder in air; (b) BaO_2 in N_2; (c) 30% Zn/BaO_2 in N_2; (d) 30% Zn/BaO_2 in air.

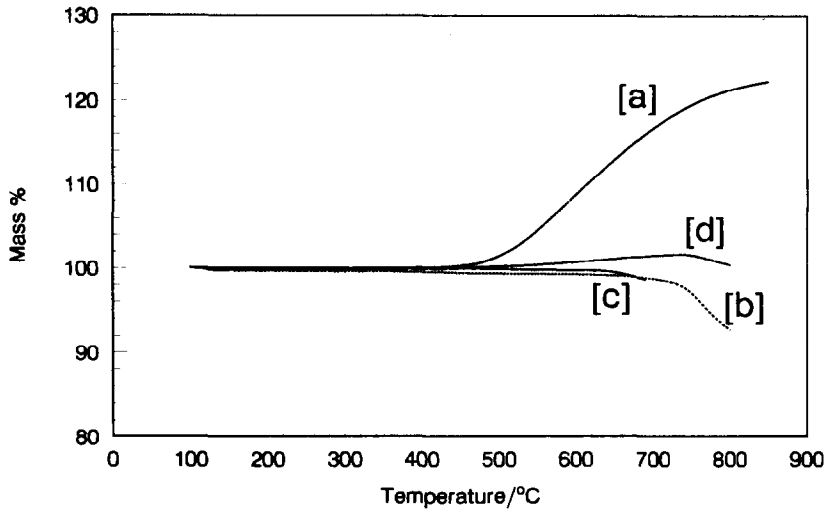

Fig. 7. TG curves for 30% Zn/BaO_2 heated at 20°C min^{-1}: (a) Zn powder in air; (b) BaO_2 in air; (c) 30% Zn/BaO_2 in N_2; (d) 30% Zn/BaO_2 in air.

mixtures in N_2. Mass loss began either at 500°C and proceeded in two steps (onsets at 500 and 560°C), or the loss began at 600°C in a single step. The mass changes observed in N_2 in the TG study may be explained in terms of the zinc vaporising from the mixture and not reacting with the peroxide. On rerunning the residue from the Zn/BaO_2 composition, which had been heated in air to 685°C and cooled in nitrogen, the DTA curve showed only a small endotherm with an onset at about 490°C. The TG curve showed a gradual mass increase, reaching a maximum of 4% at 490°C, and then decreasing to a total mass gain of 3% which was stable above 590°C.

Zn/SrO_2

The DTA curve for 30% Zn/SrO_2 heated at 20°C min^{-1} in N_2 (Fig. 8, curve c) shows two endotherms corresponding to the melting of zinc (418°C) and the decomposition of SrO_2 (onset 425°C), and a subsequent exotherm with onset at 485°C. The DTA traces in air and O_2 (Fig. 8, curve d) are almost identical to those in nitrogen, so reaction is independent of atmosphere. For a mixture aged for 24 h in air at 25°C, the reaction exotherm at 485°C decreased in size and the broad exotherm increased. The DTA curves for Zn in air (curve a) and SrO_2 in N_2 (curve b) are shown on the same scale for comparison. For the 50% Zn/SrO_2 mixture, a broad exotherm with a peak at 790°C was observed. DSC results were similar and pelleting the sample consolidated and sharpened the exotherms.

The TG curve for 30% Zn/SrO_2, heated at 20°C min^{-1} in N_2 (Fig. 9, curve c) shows a total mass change of 7.5% occurring in at least three stages: two of the stages (onsets at 435 and 570°C) are related to the decomposition of strontium peroxide, and the final gradual mass gain at the high temperature limit (700°C) is probably the last part of the concurrent oxidation of Zn. In air (curve d), the total change in mass is about 6.6%, in

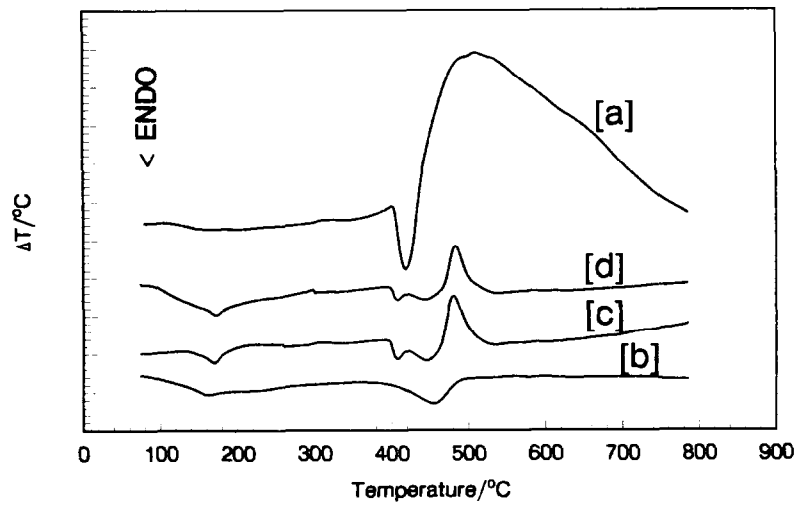

Fig. 8. DTA curves for 30% Zn/SrO_2 heated at 20°C min^{-1}: (a) Zn powder in air; (b) SrO_2 in N_2; (c) 30% Zn/SrO_2 in N_2; (d) 30% Zn/SrO_2 in air.

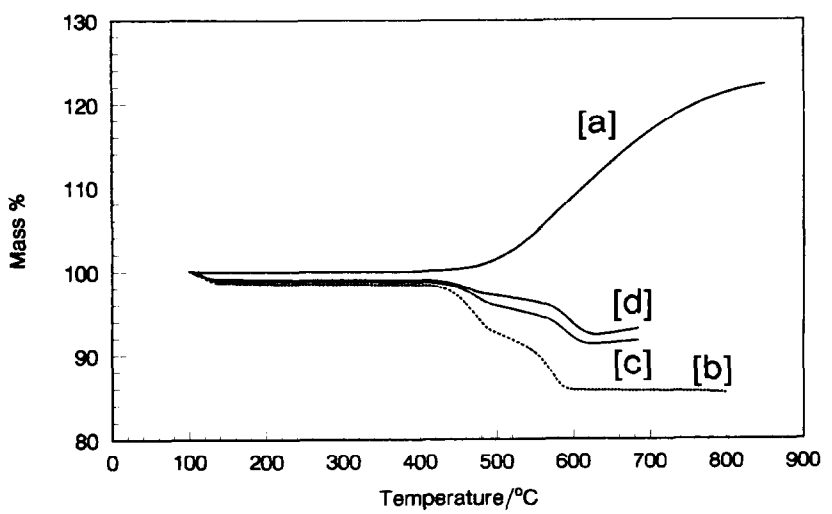

Fig. 9. TG curves for 30% Zn/SrO_2 heated at 20°C min^{-1}: (a) Zn powder in air; (b) SrO_2 in air; (c) 30% Zn/SrO_2 in N_2; (d) 30% Zn/SrO_2 in air.

similar stages to that in N_2. For the 30% Zn/SrO_2 composition, if no external reaction occurred, the overall mass change would be zero and 100% of the Zn would be oxidised. Independent oxidation of the 30% Zn (94% pure) and decomposition of the 70% SrO_2 (85% pure) would result in a net decrease in mass of 0.6%. Decomposition of

only the SrO_2 would give a decrease in mass of 8.0%. Zinc oxidation was not complete at the instrument limit and, consequently, the proportion of zinc vaporising could not be determined from the final mass of product.

$Zn/KMnO_4$

DTA curves (Fig. 10) of $Zn/KMnO_4$ mixtures show the exothermic decomposition of $KMnO_4$ at 290°C, followed by melting of zinc at 420°C. Oxidation of molten Zn then takes place. The gentle slope of this exotherm suggests that molten Zn may be reacting with residual oxygen from that liberated in the preceding decomposition, or that Zn diffuses into the products of the $KMnO_4$ decomposition, reacting within the lattice. The second stage of the oxidant decomposition then appears as an endotherm superimposed on the oxidation exotherm.

A DTA study of a 40% Zn/potassium manganate (K_2MnO_4) mixture (using K_2MnO_4 prepared from solution) heated in nitrogen showed an exotherm, similar to that in the $KMnO_4$ system, immediately after the melting of Zn. Since no oxygen had been evolved prior to this, the Zn must be diffusing into, and reacting within, the K_2MnO_4 lattice. The similarity between reaction exotherms of $Zn/KMnO_4$ and Zn/K_2MnO_4 suggests that Zn reacts primarily with the K_2MnO_4 product of the $KMnO_4$ decomposition. The onset temperature of this exotherm is significantly lower than that of the decomposition of K_2MnO_4, precluding the possibility that the initial reaction of Zn is with oxygen liberated in the decomposition of K_2MnO_4. As the temperature increases, however, Zn may react with oxygen liberated during the decomposition of K_2MnO_4.

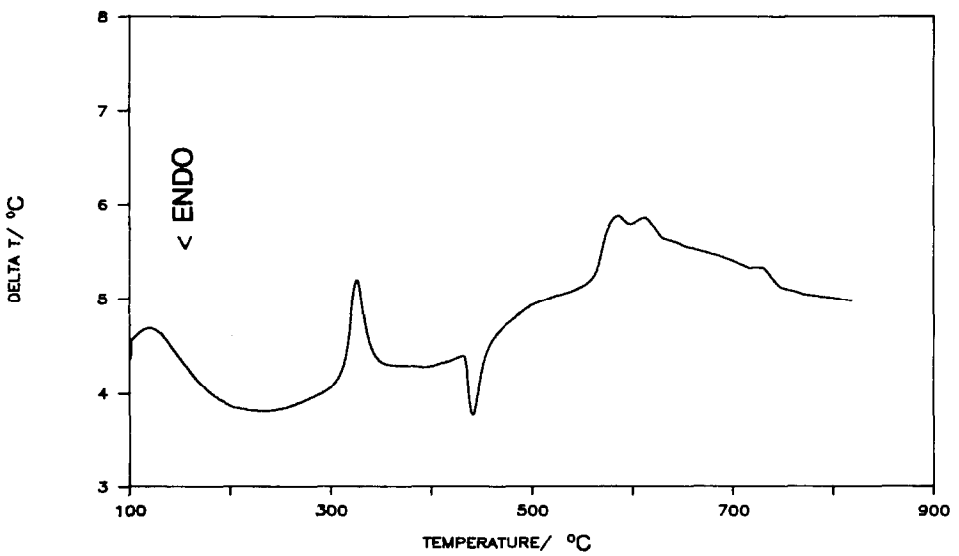

Fig. 10. DTA of 30% $Zn/KMnO_4$ heated in N_2 at 20°C min^{-1}.

A 30% $Zn/KMnO_4$ mixture was heated isothermally in nitrogen, in the DTA instrument, at 370 °C for 30 min to remove all the oxygen evolved in the first stage of the $KMnO_4$ decomposition. The mixture was then heated at 5 °C min^{-1}, and the DTA curve showed a broad, gently sloped exotherm and the endotherm corresponding to the second stage of decomposition of $KMnO_4$ at 585 °C. This supports the suggestion that Zn diffuses into the K_2MnO_4 lattice.

4. Kinetic analysis

Numerous methods have been developed to extract kinetic information from programmed temperature experiments. The Borchardt and Daniels method [23] was used in this study. The extent of reaction α at temperature T is obtained from the partial area of a DTA peak, or the fractional mass loss from a TG curve, and is used to calculate a rate coefficient k, given by $k = (d\alpha/dt)/[(1-\alpha)^n]$. The usual assumption was made that $(d\alpha/dt) = (d\alpha/dT)(dT/dt) = (d\alpha/dT)\beta$, where β, the heating rate, is held constant. The order of reaction n is then varied until a linear plot of $\ln k$ against $1/T$ is obtained, and the Arrhenius parameters, E_a and A, are calculated from the slope and intercept of the plot, respectively.

4.1. Oxidation of Zn in air

Kinetic analysis of the TG and DTA curves for the oxidation of zinc powder yielded the kinetic parameters given in Table 1. The E_a values compare satisfactorily with the literature values quoted above.

4.2. Zinc/lead oxides

DTA exotherms from mixtures of Zn with each of PbO_2, Pb_3O_4, and PbO, all recorded in nitrogen, were analysed. Kinetic parameters and values of the square of the correlation coefficient r^2 are given in Table 1. The reaction exotherm of the Zn/PbO mixture appeared to have two parts: at low temperatures (520–590 °C), the plots of $\ln k$ against $1/T$ were not very dependent on reaction order, but at higher temperatures (595–725 °C) the reaction order markedly affected the linearity of the graph.

The kinetic parameters obtained using this method of analysis show a strong dependence on the apparent order of reaction chosen. The three systems, Zn/PbO_2, Zn/Pb_3O_4 and Zn/PbO, however, gave broadly similar results in terms of the order of reaction, activation energy and frequency factor. The values of the apparent activation energies are generally higher than expected for a diffusion-type mechanism, except for the high-temperature part of the Zn/PbO reaction exotherm (57 kJ mol^{-1}). Formation of an oxide layer on the Zn could result in rate control by diffusion into the bulk of the fuel in the later stages of the reaction. This type of behaviour has been observed in the Si/PbO and B/PbO systems [1]. The apparent activation energies are also higher than the values for the oxidation of zinc by gaseous oxygen, given in Table 1. Al-Kazraji [24] found that the Borchardt–Daniels method gave results at

Table 1
Kinetic parameters obtained by analysis of DTA and TG curves using the Borchardt–Daniels method [23]

System	T range/°C	n	E_a/(kJ mol^{-1})	A/(s^{-1})	r^2
Zn					
DTA air	437–679	2	104.6±0.9	(79.02±1.7) × 10^3	0.97
TG air	395–815	2	117.1±0.7	(127.4±3.6) × 10^3	0.98
TG O_2	400–725	2	98.4±0.6	(20.7±0.4) × 10^3	0.98
Zn/Pb_3O_4	580–587	2/3	155±7	(6.7±0.1) × 10^8	0.98
Zn/PbO_2	580–594	2/3	202±12	(2.2±0.2) × 10^{11}	0.89
Zn/PbO	520–590	1	229±3	(7.9±0.5) × 10^{11}	0.99
		2	248±2	(1.4±0.1) × 10^{13}	0.99
	595–725	1	57±1	29±4	0.97
Zn/BaO_2					
DTA N_2	450–490	1	133.0±5.1	(2.48±0.01) × 10^7	0.91
		2	184.7±5.6	(1.41±0.01) × 10^{11}	0.94
DTA air	460–700	1	115.8±1.0	(4.44±0.11) × 10^4	0.96
		2	148.8±0.9	(6.74±0.10) × 10^6	0.98
DTA O_2	451–754	1	81.0±0.3	477.4±8.4	0.99
		2	136.3±1.0	(235.1±5.4) × 10^4	0.97
Zn/SrO_2					
DTA N_2	484–533	2	547.3±5.7	(24.1±0.1) × 10^{35}	0.99
DTA air	451–541	2	660±10	(12.3±0.1) × 10^{43}	0.96
DTA O_2	482–500	2	507±28	(13.7±0.1) × 10^{33}	0.90

variance with other techniques, most notably the Kissinger method, which is based on comparison of thermal analysis curves obtained at a series of different heating rates. As heating rate is an important factor in determining whether or not ignition of pyrotechnic compositions occurs under the relatively controlled conditions of thermal analysis, the Kissinger method is less likely to produce reliable kinetic information.

4.3. *Zinc/peroxides*

The extraction of kinetic data from DTA curves of the zinc/peroxide systems was complicated by the occurrence of overlapping reaction exotherms in the 420–600°C region of the Zn/barium peroxide system, and by the development (with ageing) of a broad, high-temperature exotherm in the Zn/strontium peroxide system. The kinetic parameters obtained by analysis of DTA curves of zinc powder and Zn/BaO_2 and Zn/SrO_2 mixtures by the Borchardt–Daniels method are given in Table 1. Values were very dependent on the "order of reaction" n chosen. Comparison based on a common value of $n = 2$ showed that E_a values for the reaction of Zn/BaO_2 systems in oxygen lay between values obtained in nitrogen (similar to values in air) and the value for the oxidation of Zn in oxygen. This suggests that, for the composition heated in oxygen, zinc is being oxidised simultaneously by the solid oxidant and the gaseous atmosphere to yield an average E_a value.

E_a values for the reaction of Zn/SrO_2 systems were all very much higher than those for the Zn/BaO_2 systems (Table 1), which supports the suggestion that different mechanisms operate in the reactions of the two peroxides.

4.4 *Zinc/potassium permanganate*

No TG or DTA curves suitable for kinetic analysis were obtained.

5. Conclusions

The oxidation of zinc in air begins immediately after the fusion of the metal at 420 °C. Although the standard boiling point of zinc is 908 °C, the vaporisation of zinc occurs readily above 700 °C in nitrogen.

Reactions of zinc with the solid oxidants, under the controlled heating rate conditions of thermal analysis, all show prior melting of the zinc and possibly concurrent reaction with air. Under the uncontrolled conditions of combustion, it is probable that reaction involves both molten and gaseous zinc. Mechanisms of combustion of the above pyrotechnic systems are discussed in a further paper [25].

It is important in industrial applications, such as the use of delay fuses in sealed containers, to ascertain whether the reactions of pyrotechnic compositions occur in the condensed phase, or with participation of gas formed by prior decomposition of the oxidant. Combustion studies on the above binary pyrotechnic compositions [25] suggest that zinc-fuelled pyrotechnic systems, even if they have desirable environmental properties compared with heavy metals, are unlikely to prove suitable for delay applications on account of the gassy nature of the reaction.

Acknowledgements

The authors are indebted to Dr R.A. Rugunanan for his interest and comments, and to AECI Explosives Ltd for financial support.

References

[1] P.G. Laye and E.L. Charsley, Thermochim. Acta, 120 (1987) 325.
[2] S. Gordon and C. Campbell, Proc. 5th Symp. on Combustion, Reinhold, New York, 1955, pp. 277–284.
[3] G. Krien, Explosivstoffe, 13 (1965) 205.
[4] R.C. Weast (Ed.), Handbook of Chemistry and Physics, CRC Press, 67th edn., 1987.
[5] R.F. Barrow, P.G. Dodsworth, A.R. Downie, E.A.N.S. Jeffries, A.C.P. Pugh, F.J. Smith and J.M. Swinstead, Trans. Faraday Soc., 51 (1955) 1354.
[6] A.F. Trotman-Dickenson (Ed.), Comprehensive Inorganic Chemistry, Vol. 3, Pergamon Press, Oxford, 1973, p. 187.
[7] W.J. Moore and J.K. Lee, Trans. Faraday Soc., 47 (1951) 501.
[8] J. Thomas, J. Phys. Chem. Solids, 3 (1957) 229.

[9] J.O. Cope, Trans. Faraday Soc., 57 (1961) 493.
[10] H.G. Von Schnering and R. Hoppe, Z. Anorg. Allg. Chem., 312 (1961) 87.
[11] U. Spitsbergen, Acta Crystallogr., 13 (1960) 197.
[12] H.G. Von Schnering, R. Hoppe and J. Zemann, Z. Anorg. Allg. Chem., 305 (1960) 241.
[13] M.E. Derevyaga, L.N. Stesik and E.A. Fedorin, Fiz. Goreniya Vrzryva, 13 (1977) 852.
[14] M.I. Gallibrand and B. Halliwell, J. Inorg. Nucl. Chem., 34 (1972) 1143.
[15] M.J. Tribelhorn and M.E. Brown, Thermochim. Acta, 255 (1995) 143.
[16] M. Blumenthal, J. Chem. Phys., 31 (1934) 489.
[17] Y. Azuma, M. Mizuide and K. Suehiro, Gyp. Lim., 162 (1979) 175.
[18] J.A. Hedvall, Z. Anorg. Allg. Chem., 104 (1918) 163.
[19] F.H. Herbstein, G. Ron and A. Weissman, Proc. 3rd ICTA, Vol. 2 (1971) 281.
[20] F.H. Herbstein, G. Ron and A. Weissman, J. Chem. Soc. A., (1971) 1821; J. Chem. Soc. Dalton Trans., (1973) 1701.
[21] M.E. Brown, M.J. Tribelhorn and M.G. Blenkinsop, J. Therm. Anal., 40 (1993) 1123.
[22] S.R. Yoganarasimhan, N.S. Bankar, S.B. Kulkarni and R.G. Sarawadekar, J. Therm. Anal., 21 (1981) 283.
[23] H.J. Borchardt and F. Daniels, J. Am. Chem. Soc., 79 (1957) 41.
[24] S.S. Al-Kazraji, Fast combustion reactions of silicon and lead oxide, PhD Thesis, Polytechnic of Wales, Pontypridd, UK, 1979.
[25] M.J. Tribelhorn, D.S. Venables and M.E. Brown, Thermochim. Acta, 256 (1995) 309.